

# The effect of crystallinity on the fracture of polytetrafluoroethylene (PTFE)

Eric N. Brown<sup>a,\*</sup>, Philip J. Rae<sup>a</sup>, E. Bruce Orler<sup>b</sup>, George T. Gray III<sup>a</sup>, Dana M. Dattelbaum<sup>c</sup>

<sup>a</sup> Materials Science and Technology Division, MST-8, Los Alamos National Laboratory, MS E544, Los Alamos, NM 87545, USA

<sup>b</sup> Materials Science and Technology Division, MST-7, Los Alamos National Laboratory, MS G755, Los Alamos, NM 87545, USA

<sup>c</sup> Dynamic Experimentation and Materials Science and Technology Divisions, DX-2, Los Alamos National Laboratory, MS P952, Los Alamos, NM 87545, USA

Available online 6 October 2005

## Abstract

The extremely low coefficient of friction and biocompatibility provided by the inert nature of polytetrafluoroethylene (PTFE) have led to its application in a wide range of biological implants ranging from single component PTFE structures to sliding contact pads in complex joints. In vivo fracture has been identified as a major cause of failure in these implants. It has recently been shown that the fracture behavior of PTFE undergoes transitions from brittle-fracture below 19 °C to ductile-fracture with fibril formation and large-scale plasticity over 30 °C associated with crystalline phase transformations. In this paper the formation of fibrils and an associated increase in  $J_{IC}$  fracture toughness are revealed to be restricted by an increase in crystalline content in PTFE. [LAUR 05-2223]

© 2005 Elsevier B.V. All rights reserved.

**Keywords:** Polytetrafluoroethylene (PTFE); Fracture; Crystallinity; Phase transformation

## 1. Introduction

In vivo fracture and wear have been identified as some of the major problems leading to implant failure [1]. To alleviate this, the selection and optimization of biomaterials have necessitated a balance of trading fracture toughness for wear resistance. One of the most mechanically demanding implants is the total hip replacement (THR), which includes a polymer lining at the sliding interface between the prosthetic femoral head and socket. Early applications utilized polytetrafluoroethylene (PTFE) [2], commonly known as *Teflon*<sup>®1</sup>, for the lining due to its strength and low sliding resistance. Unfortunately, low wear behavior, compounded by tissue reaction with wear debris, has led to replacement with ultra-high molecular weight polyethylene (UHMWPE) [3]. However, PTFE continues to be widely used for implants, including ball-and-socket joint reconstructions such as the temporomandibular joint [4–6], ossicular chain reconstructions [7–9], and orbital floor reconstructions [10,11], and significant improvements have since been made in the wear resistance of PTFE [12–14].

Polytetrafluoroethylene is semi-crystalline in nature, with its linear chains adopting complicated phases within crystalline

domains. The crystalline structure exhibits two atmospheric pressure crystalline transitions at 19 °C [15] from triclinic structure to partially ordered hexagonal and at 30 °C to pseudohexagonal [16]. Failure has been shown to be phase dependent with transitions from brittle-fracture below 19 °C to ductile-fracture with fibril formation and large-scale plasticity over 30 °C [17].

Two studies on the fracture behavior of well-characterized, pedigreed PTFE 7C have recently appeared in the literature [17–19]. Although both studies started with pedigreed PTFE polymer manufactured from DuPont's PTFE 7C molding powder, different temperature/pressure profiles were employed for sintering of the polymer. As a result their data provide a comparison of fracture in PTFE 7C with two known pedigrees.

This enables us to compare the effect of crystallinity on fracture toughness and mechanisms. In this paper we present a review of the fracture behavior of PTFE and discuss the effect of crystallinity on fracture based on tensile measurements, DMA, and  $J_{IC}$  fracture experiments.

## 2. Experimental procedure

### 2.1. Material preparation

Four different pedigrees of PTFE 7C are discussed in this paper with three derived from PTFE 7C sintered following

\* Corresponding author. Tel.: +1 505 667 0799; fax: +1 505 667 2185.

E-mail address: [en\\_brown@lanl.gov](mailto:en_brown@lanl.gov) (E.N. Brown).

<sup>1</sup> *Teflon*<sup>®</sup> is a registered trademark of DuPont.

Table 1  
Mass fraction crystallinity values for PTFE 7C

Material	Density (kg/m <sup>3</sup> )	X <sub>c</sub> density
Virgin PTFE 7C	2168.9±0.1	53±1
Quenched	2154.8±0.1	47±1
Annealed	2188.4±0.1	60±1
Joyce PTFE 7C	2194.1±0.1	62±1

ASTM D-4894-98 (see Ref. [17]) and one investigated by Joyce and provided by G. Kirby of NSWC Dahlgren Laboratories [19], outlined in Table 1. The virgin PTFE 7C, which has been the focus of a larger program of research at Los Alamos National Laboratory (LANL) (see Refs. [17,20–23]), is 53% crystalline (characterized by density [20]). The crystalline and amorphous densities are taken to be 2300 and 2040 kg/m<sup>3</sup>, respectively. The crystallinity of the virgin PTFE 7C was modified by quenching or annealing, as described by Rae and Brown [20], and investigated in the tensile and DMA experiments discussed in the current work. Joyce examined 62% crystalline PTFE 7C (by density) [24]. To ensure valid comparisons between the fracture data collected on the 53% crystalline PTFE 7C and the tests performed by Joyce, a limited number of CT fracture tests were performed on 62% crystalline PTFE 7C provided by G. Kirby, showing excellent agreement. With the exception of SEM micrographs, all of the fracture data presented in this paper on the 62% crystalline PTFE 7C is data reported by Joyce [18,19]. Excellent reproducibility was obtained from sample to sample, with up to six samples tested under identical conditions with all of the curves overlapping providing confidence that reliable data could be obtained in a limited number of tests.

## 2.2. Tensile testing

Tensile measurements performed at LANL on 47%, 53%, and 60% crystalline PTFE 7C utilized ASTM D-638-02 Type V specimens under constant true strain-rate control ranging from  $5 \times 10^{-5}$ – $1 \times 10^{-1}$ /s for temperatures from  $-50$ – $150$  °C [20]. Small strain experiments employed straingages, while large strain experiments to failure (extensions up to 600%) utilized a video extensometer. Tensile experiments reported by Joyce [18] on the 62% crystalline PTFE 7C utilized cylindrical dog-bone specimens and a clip on extensometer providing strain measurements up to 41% true strain (50% engineering strain). Tests were performed under constant cross-head rate ranging from  $\sim 1 \times 10^{-3}$ – $10$ /s for temperatures from  $-73$ – $23$  °C.

## 2.3. Dynamic mechanical behavior

The in-phase elastic (storage) modulus  $G'$  and loss factor  $\tan \delta$  of the 47%, 53% and 60% crystalline PTFE 7C were measured as a function of temperature by DMA. Samples were analyzed in the shear mode using a Rheometrics RDS-II. Sample bars were machined to 1.5 mm thick by 10 mm wide and 15 mm long. Frequency/temperature sweeps were obtained from 0.1 to 10 Hz at 0.5% strain under a nitrogen purge from

$-150$  to melt ( $\sim 325$  °C). The shear modulus, Young's modulus, and Poisson ratio ( $\nu=0.35$  [20]) are related by

$$G = E/2(1 + \nu) \quad (1)$$

## 2.4. Fracture testing

Fracture toughness measurements were performed using compact tension (CT) specimens as defined in ASTM Standard E-1820-01 and presented in our earlier work [17]. Due to the wide range of failure behaviors exhibited by PTFE, two methods were employed for measuring crack extension: the normalization technique of the  $J$ -integral resistance curve and optical crack tip measurement. The normalization technique was proposed by Landes and Herrera [26] and has been included in ASTM Standard E-1820-01 Appendix A for elastic-plastic fracture toughness. For a full presentation of the normalization method see Brown and Dattelbaum [17]. Joyce, who made significant contributions to the development of the normalization method for metals [18], used this method for all of his experiments on the 62% crystalline PTFE 7C. To extend our work on the 53% crystalline PTFE 7C to high temperatures, when plasticity and ductile tearing, rather than rigorous crack propagation dominates, crack extension was measured optically using a digital CCD camera with a macro lens. Mixed-mode I/II fracture experiments were performed with a modified Arcan test [27] with a CT type specimen loaded with the crack at  $90^\circ$  (pure mode I),  $45^\circ$ , and  $0^\circ$  (strongly mode II) from the load line.

## 3. Results and discussion

### 3.1. Tensile testing

Uniaxial tensile experiments on the 53% and 62% crystalline PTFE 7C samples were performed and previously reported [20,18]. Representative stress–strain curves are shown in Fig. 1. In both cases, PTFE 7C exhibited significant temperature dependence with lower strain-rate dependence are reported. The modulus (Fig. 2) and yield stress (Fig. 3) show excellent agreement between the 53% crystalline PTFE 7C and Joyce's

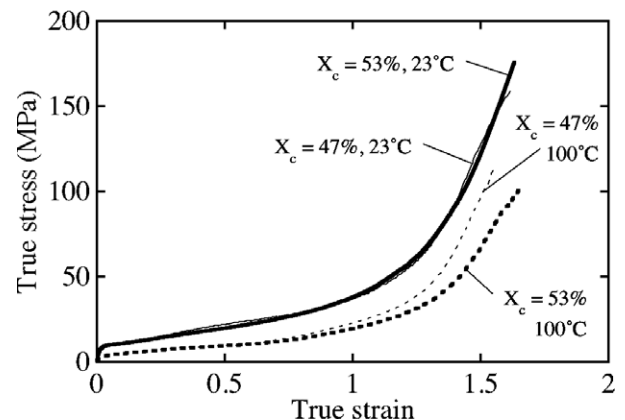


Fig. 1. Effect of crystallinity on the tensile response of 47% and 53% crystalline PTFE 7C at 23 and 100 °C [20].

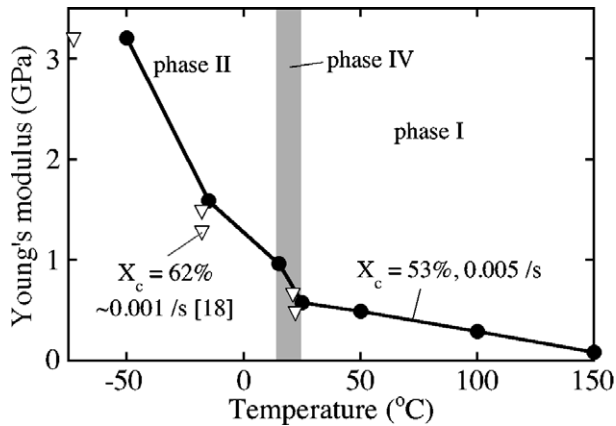


Fig. 2. Young's modulus vs. temperature for 53% and 62% crystalline PTFE 7C.

values for the 62% crystalline PTFE 7C. For small strains above yield nearly perfectly plastic deformation is observed [18]. When loaded to failure [20] PTFE 7C is characterized by immense strain to failure (approaching 600% extension in phases IV and I) with the onset of significant strain hardening without necking prior to crack initiation (Fig. 1). Meinel [28] rationalized this type of stress-strain behavior for semi-crystalline polyethylene as a physical reflection of the competition of two deformation mechanisms: initial cold drawing with rotation of the crystalline domains within the amorphous polymer maximizing crystalline chain tilt and slip, followed by orientational strengthening observed as strain hardening when available rotation and slip of the crystalline domains is diminished. Speerschneider and Li [29] reported similar phenomenon in PTFE using electron microscopy to observe crystalline regions of PTFE before and after deformation at various temperatures. Crystalline regions are initially long narrow bands with striations parallel to the long axis. In tension, the amorphous regions orient while slip occurs in the crystalline regions along the parallel striations. As slip occurs, the crystalline regions orient by rotation with the long axis along the loading direction. At higher strains, the crystals bow or kink about the striations leading to orientational strengthening. As shown in Fig. 1, a dependence on crystallinity is only observed at high-strains for elevated temperatures. The

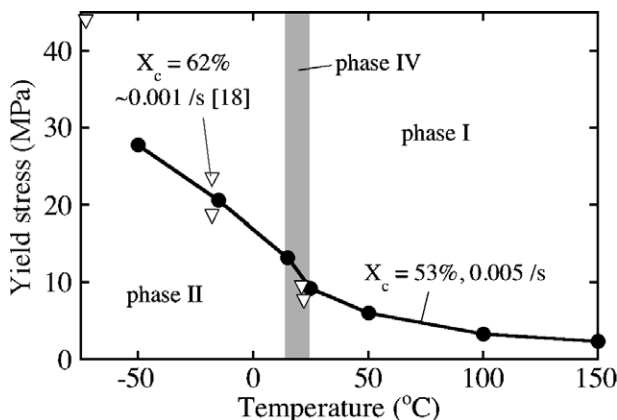


Fig. 3. Yield stress vs. temperature for 53% and 62% crystalline PTFE 7C.

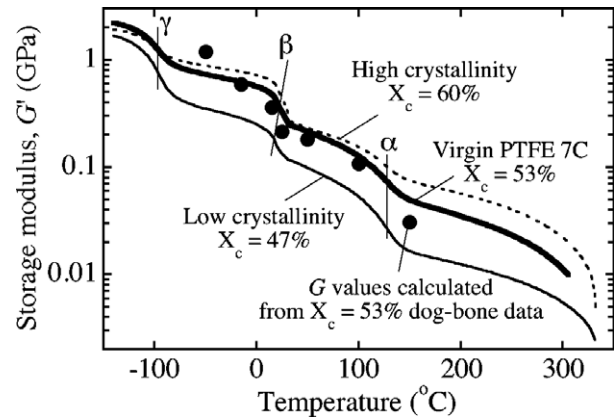


Fig. 4. Storage modulus vs. temperature for 47%, 53%, and 60% crystalline PTFE 7C with calculated shear modulus values.

observed variation for the representative curves is significantly larger than any sample-to-sample variation.

### 3.2. Dynamic mechanical behavior

General trends in the small strain elastic behavior measured by DMA (Fig. 4) exhibit similar behavior to Young's moduli measurements, with the same  $\beta$ -relaxation at 19–30 °C associated with the crystalline phase transformations. The wider range of temperatures accessed by DMA also reveals the onset of material flow due to crystalline melting above 220 °C, the  $\gamma$ -relaxation at 130 °C, and the  $\beta$ -relaxation at -95 °C. Interestingly, while decreasing the crystallinity of the PTFE 7C to 47% from the pedigreed specimens with 53% crystallinity results in a measurable decrease in modulus, increasing the crystallinity to 60% to be comparable with the PTFE 7C investigated by Joyce resulted in only a nominal increase in modulus for temperatures below the  $\gamma$ -relaxation at 130 °C, supporting the close correlation in Young's moduli for the 53% and 62% crystalline PTFE 7C shown in Fig. 2. Keeping in mind that for Eq. (1) to hold rigorously, the assumptions of classic isotropic homogeneous linear elasticity must be valid. While PTFE is semi-crystalline and nominally orthotropic, with  $E$  and  $\nu$  both dependent on direction and rate [20], the shear moduli

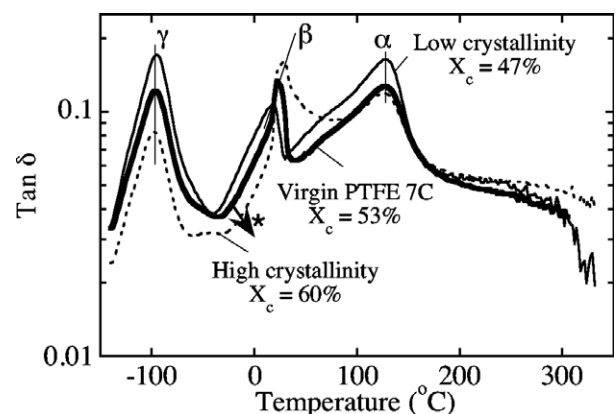


Fig. 5. Tan  $\delta$  vs. temperature for 47%, 53%, and 60% crystalline PTFE 7C.

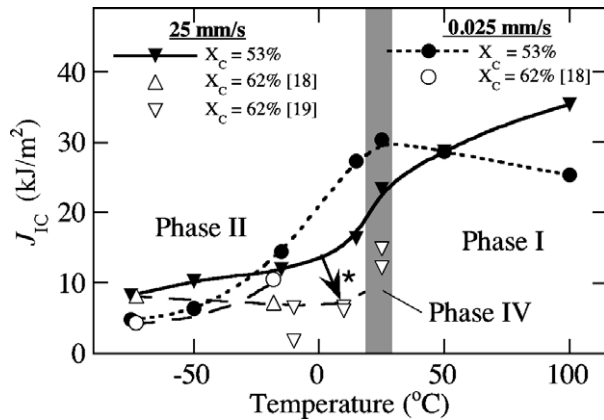


Fig. 6. Fracture toughness vs. temperature for 53% and 62% crystalline PTFE 7C.

data acquired by DMA and Young's moduli data acquired by tensile dog-bone tests are quantitatively in very good agreement in Fig. 4 with some divergence at the extreme temperatures. Error bars for the tensile data fall within the data points.

Tan  $\delta$  exhibits strong peaks associated with the  $\beta$ -relaxation at 19–30 °C associated with the phase II–IV–I crystalline transitions, the  $\gamma$ -relaxation at 130 °C, and the  $\beta$ -relaxation at –95 °C, as shown in Fig. 5, as previously reported for unspecified grades of PTFE [30–32]. Similar to the current work, Kisbenyi et al. [31] and McCrum [32] showed that the magnitude of the peaks associated with the  $\gamma$ - and  $\beta$ -relaxations in the amorphous domains is inverse to the crystallinity with negligible temperature shift. The magnitude of, and temperature for, the  $\beta$ -relaxation decrease with decreasing crystallinity. The temperature dependence may be an artifact of the  $\beta$ -relaxation being a convolution of the phase II–IV and IV–I transitions, implying that at higher crystallinities the IV–I transition leads, while at lower crystallinities the II–IV transition dominates. A subtle transition in the peaks evidenced with these transitions is observed by DSC. Moreover, while the minima between the  $\gamma$ - and  $\beta$ -relaxations are very similar in form and value independent of crystallinity, the minima between the  $\beta$ - and  $\alpha$ -relaxations takes on vastly different forms with changing crystallinity.

### 3.3. Fracture testing

Fracture behavior of the 53% crystalline PTFE 7C was measured and compared with the data reported by Joyce

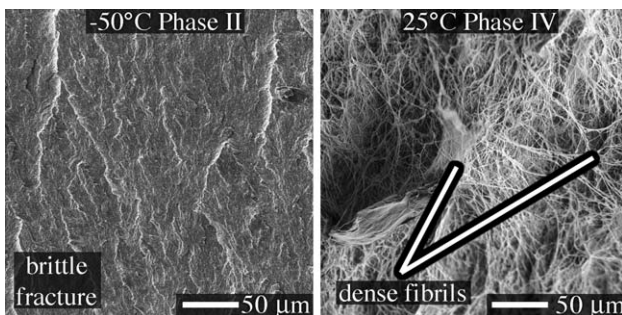


Fig. 7. SEM micrographs of the fracture plane morphology for 53% crystalline PTFE 7C in phase II and IV at 0.025 mm/s loading rate. Note: crack propagation is from bottom to top.

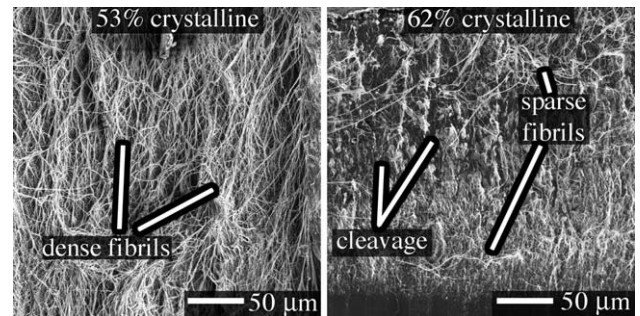


Fig. 8. SEM micrographs of the fracture plane morphology for 53% and 62% crystalline PTFE 7C in phase II at 15 °C 0.025 mm/s loading rate. Note: crack propagation is from bottom to top.

[18,19] for 62% crystalline PTFE 7C. As shown in Fig. 6, the  $J_{IC}$  fracture toughness of PTFE 7C exhibits a clear transition associated with the crystalline phase transitions. Dependence on loading rate and crystalline content are also exhibited. At low temperatures there appears to be no dependence on crystallinity, while as the temperatures approach the 19 °C phase transition the lower (40%) crystallinity PTFE 7 exhibits a much broader rise in fracture toughness while the higher (53%) crystallinity PTFE 7C offers a lower fracture toughness.

Two major mechanisms are observed for fracture of 53% crystalline PTFE 7C (as shown in Fig. 7): brittle-fracture with cleavage fracture surfaces and nominal local deformation representative of microvoid coalescence in phase II and ductile failure with significant localized deformation in the form of fibrils in phases IV and I. The formation of fibrils has previously been shown to be a key toughening mechanisms associated with the phase II–IV transition [17]. Comparison of the resulting fracture morphologies for the 53% and 62% crystalline PTFE 7C, shown in Fig. 8, indicate that the increased crystallinity of the 62% crystalline sample decreases the efficiency in fibril formation. While the 53% crystalline PTFE 7C exhibits a uniform coverage of dense fibrils on the fracture plane, the 62% crystalline PTFE 7C has only a sparse coverage of fibrils offering much less toughening and resistance to crack propagation. This is reflected by a 56% decrease in the measured  $J_{IC}$  for the case shown in Fig. 7 and the observed trend of decreased fracture toughness with increased crystallinity shown in Fig. 6 (indicated by \*).

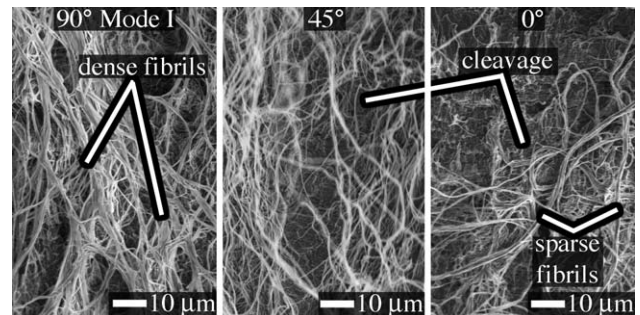


Fig. 9. SEM micrographs of the mixed-mode I/II fracture plane morphology for 53% crystalline PTFE 7C at 24 °C 0.025 mm/s loading rate. Note: crack propagation is from bottom to top.

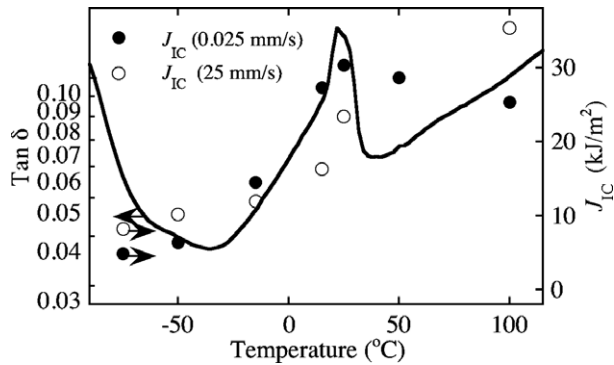


Fig. 10.  $\tan \delta$  and fracture toughness vs. temperature for 40% crystalline PTFE 7C.

A full discussion of the analysis required to quantify the mixed-mode  $J_{IC}$  fracture toughness is beyond the scope of this paper. Moreover, unlike the method for mode I  $J_{IC}$  fracture tests based on significant investigation in the literature and an ASTM standard (E-1820-01), there is currently no accepted standard for mixed-mode I/II  $J_{IC}$  measurements. Numerous papers can be found in the literature reporting on various methods for analysis and specimen geometries [27,33–35]. In the current work, we simply report changes in morphology associated with the changing load angle for the 53% crystalline material in phase IV at room temperature (24 °C). The progression of fracture plane morphologies from 90° (pure mode I) to 45° to 0° (strongly mode II) from the load line is shown in Fig. 9. In pure mode I a dense network of fibrils is observed, Fig. 7. As the mode-mixity of crack tip loading transitions to stronger mode II (shear) loading the fibrils become sparse with an increased presence of cleavage.

The potential for  $\tan \delta$  to provide an indicator for polymer impact fracture toughness has been proposed in the literature [30,31] with the underlying argument that a material with a high  $\tan \delta$ , or a peak in  $\tan \delta$  due to temperature, possesses a higher aptitude to dissipate energy through internal mechanisms other than damage or fracture. These materials would therefore exhibit higher fracture toughness because only a small portion of the total input energy would be available for crack propagation. Some effort has been made to extend the correlation of impact fracture toughness with  $\tan \delta$  to fracture and fatigue of polymers [36,37]. However, attempts to correlate fracture toughness directly with  $\tan \delta$  have had limited success [38]. In general only complex qualitative interpretation has been made and Vincent [30] has shown that at best the statistical significance of changes in  $\tan \delta$  account for two-thirds of the variance in fracture toughness. While  $\tan \delta$  clearly provides insight into a material's ability to dissipate energy, which is a critical contributor to its fracture behavior, it provides no insight into the actual mechanisms of crack initiation or growth and ignores other contributing factors such as rate, inertia, crazing, crack bridging, morphology, etc. Fig. 10 shows the qualitative correlation of  $\tan \delta$  and  $J_{IC}$ . While the increase in fracture toughness with temperature from phase II into phase IV is reasonably captured, especially for the 0.025 mm/s data, the measured fracture toughness did not follow the

$\tan \delta$  trends for the phase IV–I transition or the increase in  $\tan \delta$  at low temperature associated with the  $\gamma$ -relaxation. It is not surprising that there is poor agreement at the higher temperatures in phase I where fibril formation is a dominant mechanism. Interestingly the  $\tan \delta$  data shown in Fig. 5 shows that the onset of the peak  $\tan \delta$  with temperature at the phase II–IV transition is retarded by an increase in crystallinity (indicated by \*). The same trend for a decrease in fracture toughness with increased crystallinity is witnessed in the fracture data shown in Fig. 6 (also indicated by \*).

#### 4. Conclusions

Fracture toughness of PTFE 7C was measured over a range of temperatures and several percent crystallinities to systematically interrogate failure mechanisms. Mode I fracture of PTFE 7C undergoes transitions from brittle-fracture below 19 °C to ductile-fracture with fibril formation associated with the phase II–IV crystalline transformation, to large-scale plastic drawing and deformation at 30 °C associated with the phase I above the IV–I phase transition temperature. Comparison of 53% and 62% crystalline PTFE 7C showed nominal changes in the small strain behavior by tensile dog-bone tests with these observations confirmed by DMA. However, the formation of fibrils and associated increase in  $J_{IC}$  are restricted by the increase in crystallinity. Qualitative comparisons of the fracture toughness and  $\tan \delta$  showed similar behavior for the phase II–IV crystalline transformation, both exhibiting decreases with increased crystallinity. This is attributed to diminished fibril formation and molecular mobility with higher crystalline content. A decrease in fibril formation also occurred when the mode-mixity of crack tip loading transitioned from pure mode I (tension) towards mode II (shear). This is because fibril formation is a unidirectional process, which is diminished by the addition of shear.

#### Acknowledgements

This research was supported under the auspices of the US Department of Energy operated by the University of California. Specifically, this work was supported, in part, by the joint DOE/DoD Office of Munitions Memorandum of Understanding lead by B. Clements, of the Los Alamos National Laboratory (LANL). E.N. Brown acknowledges the Los Alamos National Laboratory Director's Funded Postdoctoral Fellowship program for support. The authors thank G. Kirby of NSWC Dahlgren Laboratories for helpful technical input and providing the higher crystallinity PTFE 7C material. Micrographs were acquired at the Electron Microscopy Laboratory (LANL) on a JEOL JSM-6300FXV.

#### References

- [1] S.H. Teoh, *Int. J. Fatigue* 22 (2000) 825.
- [2] H.R. Piehler, *MRS Bull.* 25 (2000) 67.
- [3] L.A. Pruitt, *Biomaterials* 26 (2005) 905.
- [4] K. Messner, J. Gillquist, *Biomaterials* 14 (1993) 513.

- [5] L.M. Wolford, Oral Surg. Oral Med. Oral Pathol. Oral Radiol. Endo. 83 (1997) 143.
- [6] L.G. Mercuri, A. Giobbie-Hurder, J. Oral Maxillofac. Surg. 62 (2004) 1088.
- [7] G. Geyer, HNO 47 (1999) 77.
- [8] A. Neumann, K. Jahnke, Mater.Wiss. Werkst.Tech. 34 (2003) 1052.
- [9] H.P. Zenner, H.G. Freitag, C. Linti, et al., Hear. Res. 192 (2004) 36.
- [10] R. Kontio, R. Suuronen, O. Salonen, et al., J. Oral Maxillofac. Surg. 30 (2001) 278.
- [11] E. Ellis III, E. Messo, J. Oral. Maxillofac. Surg. 62 (2004) 873.
- [12] W.P. Phipatanakul, S.A. Johnson, V. Good, I.C. Clarke, J. Biomed. Mater. Res. 39 (1998) 229.
- [13] I.C. Clarke, F.W. Chan, A. Essner, et al., Wear 250 (2001) 188.
- [14] J.Q. Yao, M.P. Laurent, T.S. Johnson, C.R. Blanchard, R.D. Crowninshield, Wear 255 (2003) 780.
- [15] C.W. Bunn, E.R. Howells, Nature 174 (1954) 549.
- [16] C.A. Sperati, H.W. Starkweather Jr., Advances in Polymer Science, vol. 2, Springer-Verlag, Berlin, 1961, p. 465.
- [17] E.N. Brown, D.M. Dattelbaum, Polymer 46 (2005) 3056.
- [18] J.A. Joyce, Polym. Eng. Sci. 43 (2003) 1702.
- [19] P.J. Rae, J.A. Joyce, Int. J. Fract. 127 (2004) 361.
- [20] P.J. Rae, E.N. Brown, The properties of poly(tetrafluoroethylene) (PTFE) in Tension, Polymer 46 (2005) 8128.
- [21] P.J. Rae, D.M. Dattelbaum, Polymer 45 (2004) 7615.
- [22] N.K. Bourne, G.T. Gray III, J. Appl. Phys. 93 (2003) 8966.
- [23] P.J. Rae, E.N. Brown, B.E. Clement, D.M. Dattelbaum, Pressure induced phase change in poly(tetrafluoroethylene) at modest impact velocities, J. Appl. Phys. 98 (in press).
- [24] The 62% crystallinity value reported here for Joyce's PTFE were measured by the authors using density on a sample of PTFE provided by G. Kirby of NSWC Dahlgren Laboratories from the same process as provided to Joyce. Crystallinities as reported by Joyce [19] were attributed to Kirby et al. [25] citing personal communication with Dattelbaum and Orler at LANL for a different pedigree of PTFE 7C than studied by Joyce.
- [25] G. Kirby, R. Garret, C. Dyka, Review of Process in Modeling Constitutive, Damage and Fracture Behavior of PTFE Subjected to Dynamic Loading, Presented at International Conference on Plasticity, 2003.
- [26] J.D. Landes, R. Herrera, Int. J. Fract. 36 (1988) R9.
- [27] Y. Arun Roy, R. Narasimhan, P.R. Arora, Acta Mater. 47 (1999) 1587.
- [28] G. Meinel, A. Peterlin, J. Polym. Sci. 9 (Pt. A-2) (1971) 67.
- [29] C.J. Speerschnieder, C.H. Li, J. Appl. Phys. 34 (1963) 300.
- [30] P.I. Vincent, Polymer 15 (1974) 111.
- [31] M. Kisbenyi, M.W. Birch, J.M. Hodgkinson, J.G. Williams, Polymer 20 (1979) 1289.
- [32] N.G. McCrum, J. Polym. Sci. 34 (1959) 355.
- [33] M.A. Sutton, X. Deng, R. Ma, et al., Int. J. Solids Struct. 37 (2000) 3591.
- [34] C.D. Donne, A. Pirondi, J. Test. Eval. 29 (2001) 239.
- [35] S.M.A. Khan, M.K. Khraisheh, Int. J. Plast. 20 (2004) 55.
- [36] J. Kargerkocsis, V.N. Kuleznev, Acta Polym. 33 (1982) 14.
- [37] P. Faughnan, C. Bryan, Y. Gan, H. Aglan, J. Mater. Sci. Lett. 17 (1998) 1743.
- [38] R.M. Evans, H.R. Nara, R.G. Bobalek, Soc. Plast. Eng. 16 (1960) 76.